Mausam, (1985), **36**, 2, 127-134

551.509.327 : 551.509.313

Certain aspects on the realization of primitive equations forecasting model in the low latitudes

U. C. MOHANTY and FLT. LT. S. C. MADAN*

Centre for Atmospheric & Fluids Sciences, Indian Institute of Technology, New Delhi

(*Received 27 January 1983*)

सार — उष्ण कटिबन्धीय प्रणालियों के पूर्वानुमानों के लिये एक दाब घनत्वी पूर्वग समीकरण मॉडल के साथ कई आंकिक प्रयोग किए गए थे। निम्न अक्षांशों में ऐसे साधारण पू०स०मॉडल की समन्वय-प्रक्रिया में आई कुछ महत्वपूर्ण समस्याओं के समाधान के लिये विधिवत् प्रयास किया गया है। कटिबन्धों में आरंभिक आंकड़ा समस्या पर अधिक जोर दिया गया है। पूर्वानुमान मॉडल पर गतिकीय इनीशियलाइजेशन तथा फिलटरन तकनीकों के प्रभाव का अध्ययन करने के लिये तथा फिलटरन तकनीकों के समरेखण गुणों के अध्ययन के लिये इनिशियल, इनिशियलाइज्ड, पूर्वानुमानित तथा वास्तविक पवन क्षेत्रों की गतिज ऊर्जा का मानावलीय विनियोजन किया गया है। तदन्तर, इन तकनीकों के उपयोग से मॉडल की कार्यक्षमता में आए सुधार को दर्शाया गया है। अन्तिम रूप से इस मॉडल को बंगाल की खाड़ी में कटिबन्धीय चक्रवातों की गति तथा मानसून अवदाब के पूर्वानुमान के लिये इस्तेमाल किया गया है। इस मॉडल की सीमाओं के बावजूद उसके परिणाम काफी उत्साहवर्धक है।

ABSTRACT. A number of numerical experiments are carried out with a barotropic primitive equations (PE) model for forecasting the tropical systems. A systematic approach has been made to solve some of the important problems arising in the process of integrating such a simple PE model in the low latitudes. Emphasis has been given to the initial data problem in the tropics. In order to study the influence of dynamical initialization and filtering techniques on the forecasting model and to study their smoothing characteristics, the spectral decomposition of kinetic energy of initial, initialized, forecast and actual wind fields, is carried out. Further, the improvement in the efficiency of the model by incorporating these techniques is demonstrated. Finally, this model is applied to forecast the movement of tropical cyclones and a monsoon depression in the Bay of Bengal and inspite of the constraints of the model, the results are quite encouraging.

1. Introduction

Most of the numerical prediction models (filtered and PE models) developed for the mid-latitude, make use of the observed geopotential field as initial data, because this field is comparatively smoother, more accurate in measurement in mid-latitudes and easier to analyse than the wind field. The velocity field is obtained from geopotential field by using geostrophic balance. However, the realization of initial data by this process in the tropics is more difficult as :

(*i*) Nearly 2/3 of the tropical belt is covered with data sparse oceanic region.

(*ii*) In the tropics, the gradient of geopotential is very small and also the day to day variability is of the same order as the inherent observational error. Further, the geostrophic relation does not hold good and the solution of the balance equation suffers from ellipticity problems.

From the above it is clear that the use of geopotential height as the basic input to the prediction models in the tropics, has certain serious practical and theoretical limitations. Whereas, the wind field, as found from theoretical and model considerations, seems to be the better source of data in the tropics (Obukhov 1949, Winninghoff 1968, Houghton and Washington 1969, Gordon *et al.* 1972), it suffers from sparsity of observational network. Efforts are continuing to increase the density of observations in the tropics. One of the main purpose of First GARP Global Experiment (FGGE) was to evaluate the performance of the models with the increase in density of observations in the tropics. With the introduction of geostationary satellites with meteorological payloads, the wind field can be derived from the cloud movement more accurately for the tropical regions than for the polar latitudes.

Inspite of enhancement of wind observations by geostationary satellites, choice of wind field as basic data suffers from the problem of objective analysis at regular grid points and estimation of geopotential height by solving non-linear balance equations, which require the knowledge of stream functions (Mohanty and Madan 1983).

Therefore so far, there is no single and unique opinion in favour of either wind or geopotential height data, for their use as the initial data in the tropisc.

Directorate of Meteorology, Air HQs, Vayu Bhavan, New Delhi-110011

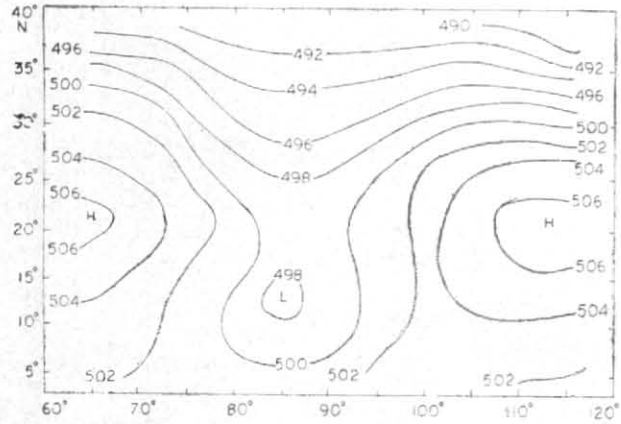

Fig. 1. Initial geopotential field (dkm) for 6 Nov 1973

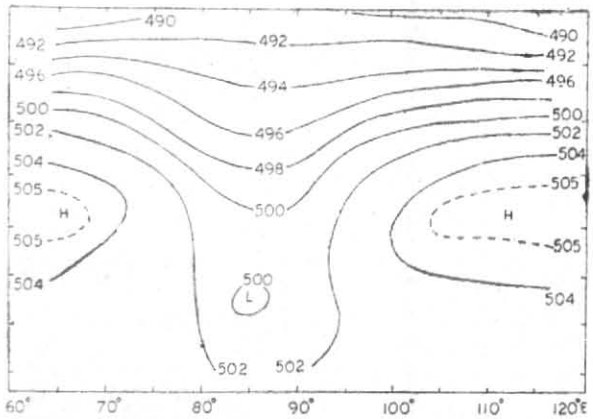

Fig. 2. Initialized geopotential field (dkm) for 6 Nov 1973, obtained after 18 hours initialization

Some of the works (Falkovich 1971, Krichak 1976, Das and Bedi 1978) used geopotential field as the input data in their models, whereas others (Vanderman 1969, Krishnamurti 1969, Gordon *et al.* 1972) used wind field. Thus, it is revealed that the initial data problem in the tropics requires further systematic studies.

Besides this, the integration of a PE model is encountered with other problems, *i.e.*, initialization of mass and velocity fields, smoothing and filtering of high frequency waves. In this study, a number of experiments have been carried out with a PE barotropic model to demonstrate the problems involved with the practical realization of this model in the low latitudes and their possible solutions.

2. Model

2.1. *Basic equations*— In this study, a barotropic PE model is used for a limited area mercator projection of the tropical belt, bounded by 3°–40° N and 60°–120° E.

The basic equations of the barotropic PE model in cartesian coordinates on mercator projection are :

$$\frac{\partial u}{\partial t} - fv + m\left(u\frac{\partial u}{\partial x} + v\frac{\partial u}{\partial y} + g\frac{\partial h}{\partial x}\right) = 0 \qquad (1)$$

$$\frac{\partial v}{\partial t} + fu + m\left(u\frac{\partial v}{\partial x} + v\frac{\partial v}{\partial y} + g\frac{\partial h}{\partial y}\right) = 0 \qquad (2)$$

$$\frac{\partial h}{\partial t} + m\left[u\frac{\partial h}{\partial x} + v\frac{\partial h}{\partial y} + h\left(\frac{\partial u}{\partial x} + \frac{\partial v}{\partial y}\right)\right] - hv\frac{\partial m}{\partial y} = 0 \qquad (3)$$

where, m — the map factor ($m = \sec\phi$, where ϕ is the latitude at which the projection is true).

All the other variables have their usual meaning.

2.2. *Boundary conditions* — The rigid walls are imposed at the northern and southern boundaries (*i.e.*, $v=0$). Applying this assumption in the momentum equations (Eqns. 1-2), the boundary conditions for u and h are obtained. Thus at the north and south boundaries :

$$v = 0 \qquad (4)$$

$$\frac{\partial u}{\partial t} + m\left(u\frac{\partial u}{\partial x} + \frac{\partial}{\partial x}(gh)\right) = 0 \qquad (5)$$

$$fu + m\frac{\partial}{\partial y}(gh) = 0 \qquad (6)$$

At the eastern and the western ends, cyclic conditions are imposed. This type of boundary conditions are used by Shuman and Vanderman (1969), and Kivganov and Mohanty (1979).

3. Numerical solution

Shuman's semi-momentum finite difference scheme (Shuman 1962) is used to evaluate the space derivatives in the Eqns. (1)-(3), (5) & (6). Euler — backward finite difference scheme is employed at the first time step, while Adams-Bashforth scheme is employed in the successive time steps.

Since the domain of integration is divided into a number of regular grid points with spacing of 210 km, the time steps of 5 minutes are found to be suitable.

4. Data

For this study, a typical synoptic situation dominated by a tropical severe cyclonic storm in the Bay of Bengal (6 and 7 Nov 1973), has been selected. Analysis of wind field (stream lines and isotachs) and geopotential field (contour analysis) was carried out manually for 6 mandatory pressure levels (1000, 850, 700, 500, 300 and 200 mb) at 0000 GMT. It is suggested by Sanders *et al.* (1975) that a vertical integration of the flow pattern in the tropics is a better representation of the tropical cyclone and its movement by barotropic models.

With this consideration, in this work the pressure weightage averages of u, v and h fields are carried out

TABLE 1

Results of the spectral decomposition of KE in the process of initialization (6 Nov' 73)

Wave No.	Initial (6' Nov)	During the process of initialization 6 hr	12 hr	18 hr	24 hr
$m=0$ (Zonal k_o)	34.5	34.3 (0.5)	34.2 (0.7)	34.1 (0.9)	34.1 (0.9)
$m=1, 2$ (Long waves) $L \geqslant 3400$ km	6.9	6.2 (10.7)	6.1 (11.5)	6.1 (12.0)	6.0 (12.4)
$m=3, 6$ (Synoptic scale) $L \geqslant 1100$ km < 3400 km	0.5	0.4 (27.8)	0.4 (29.4)	0.4 (30.1)	0.4 (30.5)
$m=7, 15$ (Short waves) $L \geqslant 420$ km < 1100 km	0.2	0.1 (42.5)	0.1 (46.2)	0.1 (48.7)	0.1 (50.3)
$m=0, 15$ Total k_t	42.1	41.0 (2.7)	40.8 (3.1)	40.7 (3.3)	40.6 (3.5)
$\frac{k_o}{\text{Total } k_t}$	0.82	0.84	0.84	0.84	0.84

Note : The figures in brackets give the % change from the initial values

over the atmospheric layer between 1000 and 200 mb levels by the relation :

$$\bar{X} = \int_{1000}^{200} X\,dp \Big/ \int_{1000}^{200} dp \quad , \quad \text{where } X = (u, v\ h) \tag{7}$$

Similar type of fields are also used by Gandin (1963). Vertically averaged geopotential fields for 6 and 7 Nov '73 at 0000 GMT are given in Figs. 1 and 5.

5. Numerical experiments

The following numerical experiments have been carried out to demonstrate some of the problems involved with the practical realization of a PE model in the tropics.

5.1. *Static initialization*

The wind field is considered as the basic input to the model (Eqns. 1-3). In order to evaluate the geopotential height from the observed wind fields, the following steps are taken :

(*i*) The stream function ψ is obtained from the observed wind field (Mohanty and Madan 1983).

(*ii*) The geopotential height is obtained from the non-divergent wind fields by the iterative solutions of the non-linear reverse balance equation :

$$\nabla^2 (h) = -\frac{1}{g}\left[\nabla.(\mathbf{V}_\psi.\ \nabla \mathbf{V}_\psi) - \frac{1}{m}\,\mathbf{k}.\left\{ \nabla \times (f\mathbf{V}_\psi) \right\}\right] \tag{8}$$

where, $u_\psi = -\dfrac{\partial \psi}{\partial y} \quad v_\psi = \dfrac{\partial \psi}{\partial x}$

In the solution of Eqn. (8), the observed values of geopotential height are taken as the boundary values and the space derivatives are discretized by Shuman's semi-momentum finite difference scheme.

Mean absolute difference $|\overline{\delta H}|$ between the observed and the derived geopotential and their maximum difference $|\delta H|_m$ are calculated for both the synoptic cases in order to evaluate the accuracy and representativeness of the derived geopotential field. It is found that mean $|\overline{\delta H}|$ is 0.7 decametre whereas mean $|\overline{\delta H}|_m$ is 3.7 decametres. Mean absolute maximum difference is observed close to the cyclonic centre. From this experiment, it may be concluded that the derived geopotential heights from the observed winds in the tropics can be used as the initial data with reasonable accuracy.

5.2. *Dynamic initialization*

The method of dynamic initialization used is similar to that proposed by Nitta and Hovermale (1969) and applied earlier to tropics by Mohanty (1982). A number of numerical experiments have been carried out in this study to provide an elaborate illustration of the impact of dynamic initialization on numerical weather prediction in the tropics.

These numerical experiments are broadly divided into three categories :

(*i*) To ascertain the reliability and acceptance of the initialized fields as input in the model.

(*ii*) To study the impact of initialization in the process of integration of the model.

(*iii*) To evaluate the role of initialization on the 24 hours forecasting parameters.

In order to evaluate the reliability of the initialized u, v and h fields, the initial observed wind (u, v), and geopotential (h) derived from u and v, by static initialization for 6 Nov'73, are subjected to dynamic initialization (18 hours pseudo forecasting). The mean absolute differences $|\overline{\delta H}|$, $|\overline{\delta u}|$, $|\overline{\delta v}|$ between the initial fields and the initialized fields are calculated. It is found that after 18 hours of initialization, these mean absolute differences are 0.7 decametre, 1.3 m/sec and 1.1 m/sec respectively. Further, for a qualitative comparison, the 18 hours initialized geopotential field for 6 Nov '73 is illustrated in Fig. 2. It is evident from Figs. 1 and 2 that though the broad features and the positions of cyclonic and anticyclonic centres are unaltered during the process of initialization, the initialized h field is smoothed to some extent. The geopotential height of the cyclonic centre is risen by 2 decametres and there is a decrease of h by one decametre at both the anticyclonic centres.

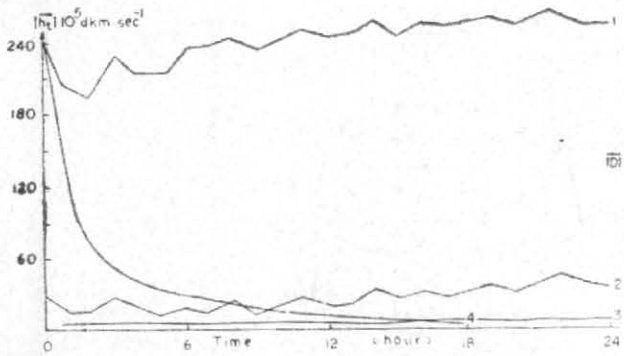

Fig. 3. Time tendency of geopotential during: (1) Forecast without initialization, (2) Forecast after 6 hours initialization, (3) Forecast after 18 hours initialization, and (4) 18 hours initialization process

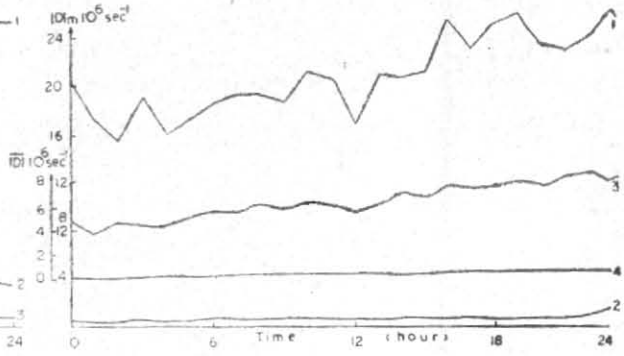

Fig. 4. Maximum and mean divergence fields during : (1), (3) : Forecast without initialization, (2), (4) : Forecast after 18 hours of initialization

Thus from both the quantitative and the qualitative evaluations, it may be concluded that the meteorological fields do not undergo any radical changes during the process of dynamic initialization, which may be due to the fact that the mechanism of initialization mainly suppresses only the high frequency gravity modes, without any substantial change to the broad synoptic scale processes.

In order to investigate the above statement, the spectral decomposition of kinetic energy (Cooley and Tukey 1965) of initial wind (u, v) and the initialized wind with different periods of pseudo forecasting (6, 12, 18 and 24 hours) are given in Table 1. Kinetic energy and its percentage variations (given in brackets) from the initial wind fields are computed over the entire spectrum of the waves and are grouped in to four categories such as zonal (wave number $m=0$), long waves ($m=1$-2), synoptic scale waves ($m=3$-6) and short waves ($m=7$-15).

From the analysis of Table 1, it becomes clear that in the process of dynamic initialization the change in the total kinetic energy does not exceed 4% of its initial value. Kinetic energy for zonal motions (wave number $m=0$), which is about 84% of the total kinetic energy, practically remains same as that of the initial wind, as the maximum percentage variation is only 0.9%. While kinetic energies of long waves, synoptic waves and high frequency waves decrease by about 12, 30 and 50 % respectively. Thus the initialization procedure shows the properties of selective reduction of the amplitudes of the different modes with maximum reduction for short waves and minimum for zonal waves. It is found that most of the reduction of kinetic energy over the entire spectrum, takes place during the first 6 hours, which is the characteristic period of geostrophic adaptation of the mass and the velocity fields (Obukhov 1949), and with further increase in the period of initialization, changes are quite insignificant.

To study the effect of initialized fields compared to the initial fields, during the process of integration of the prediction model (Eqns. 1-3), three experiments are conducted with (*i*) initial fields (without initialization), (*ii*) initial field after 6 hours of initialization and (*iii*) initial field after 18 hours of initialization. As a barotropic PE model is isolated from external sources of energy, the values of mean absolute local rate of change of the dependant variables ($|\overline{u_t}|$, $|\overline{v_t}|$, $|\overline{h_t}|$) should be more or less stable and constant during the 24 hours forecasting period. But it is evident from Fig. 3 that during the first 6 hours period, the forecast with non-initialized fields, gives an unstable and unrealistically high values of $|\overline{h_t}|$, which is a sign of computational instability. The field with 6 hours of initialization also indicates some unusual changes of $|\overline{h_t}|$, whereas the field with 18 hours of initialization gives almost constant and realistic values of $|\overline{h_t}|$ during the entire 24 hours forecasting period. Similar trends are seen in $|\overline{u_t}|$, $|\overline{v_t}|$ values also.

Further, it is interesting to find out the change of the mean absolute divergence $|\overline{D}|$ and absolute maximum divergence $|D|_m$ in the process of 24 hours forecast, as the gravity waves manifest themselves almost entirely in the irrotational part of the fluid motion. The mean absolute divergence $|\overline{D}|$ and absolute maximum divergence $|D|_m$, over the entire prediction domain, are estimated and illustrated in Fig. 4. It is found that at initial time (time $T=0$) both $|\overline{D}|$ and $|D|_m$ for non-initialized wind fields are considerably higher than the corresponding values with the initial initialized (18 hours) winds (4 and 20 times respectively). Thus, these experiments illustrate that though the mass and the velocity fields are balanced by static initialization, they do not satisfy exact conditions of balance, when used as input variables, in the prediction model, and thus lead to the conditions of instability and also yield unrealistic high values of these meteorological fields during the process of time integration of the model. To find out the importance of dynamic initialization in numerical weather prediction, the following parameters, which are used to evaluate the efficiency of a numerical model in the prediction of meteorological variables, are estimated.

$$R_1=\left[\sum_{i=1}^{N}\left(X_{pi}-X_{ai}\right)\right]\Big/ N. \qquad (9)$$

TABLE 2

Results of evaluation of different types of forecasts from initial fields of 6 Nov 1973

Different types of initial fields	h			u			v		
	R_1	R_2	R_3	R_1	R_2	R_3	R_1	R_2	R_3
Without initialization	32.8	17.8	8.4	8.5	2.5	2.7	14.9	4.4	3.8
With initialization (without filter)	3.4	1.4	.54	2.8	.74	.72	2.9	.6	.6
With initialization and filter	2.8	1.1	.49	2.3	.72	.71	2.5	.6	.6

TABLE 3

Results of spectral decomposition of KE of the initial wind field (6 Nov' 73), actual wind field of the next day (7 Nov' 73) and forecast wind field with different level of initialization (0, 6, 18 hr of initialization

Wave No.	Initial 6 Nov 1973	24 hours forecast: Without initialization	24 hours forecast: With 6 hr initialization	24 hours forecast: With 18 hr initialization	Actual 7 Nov 1973
$m=0$ (Zonal k_0)	34.5	62.2	36.2	30.7	30.8
$m=1, 2$ (Long waves) $L \geqslant 3400$ km	6.9	13.5	9.0	5.3	7.3
$m=3, 6$ (Synoptic scale) $L \geqslant 1100$ km < 3400 km	0.5	47.1	5.8	0.5	1.4
$m=7, 15$ (Short waves) $L \geqslant 420$ km < 1100 km	0.2	7.1	1.9	0.3	0.6
$m=0, 15$ Total k_t	42.1	129.9	52.9	36.8	40.1
$\frac{k_0}{\text{Total } k_t}$	0.82	0.48	0.68	0.83	0.77

$$R_2=\left[\sum_{i=1}^{N}\left|X_{pi}-X_{Ii}\right|\right]\Big/\left[\sum_{i=1}^{N}\left|X_{ai}-X_{Ii}\right|\right] \qquad (10)$$

$$R_3=\frac{\sqrt{\sum_{i=1}^{N}\left[\left(X_{pi}-X_{Ii}\right)-\left(\overline{X_{pi}-X_{Ii}}\right)\right]^2}}{\sqrt{\sum_{i=1}^{N}\left[\left(X_{ai}-X_{Ii}\right)-\left(\overline{X_{ai}-X_{Ii}}\right)\right]^2}} \qquad (11)$$

where,

N=number of grid points over which the forecast is evaluated.

X=(u, v, h) and the suffix I, a and p, stand for initial, actual and predicted values of the meteorological field X respectively.

For an ideal forecast, the values of R_1, R_2 and R_3 should be 0, 1 and 1 respectively. Thus the efficiency of the model with different input variables can be judged by the values of these parameters in relation to their ideal values. R_1, R_2 and R_3 are estimated for two sets of 24 hours of forecasts, *i.e.*, (*i*) forecast with non-initialized variables as input, (*ii*) forecast with initialized fields as input, and are presented in Table 2. From the first two rows of Table 2, it can be inferred that the forecast with initalized fields as input is much better than the forecast with input fields without initialization.

In order to find out the efficiency of the model integrated with non-initialized and initialized input variables, to predict different scales of processes, the spectral decomposition of kinetic energy of initial, 24 hours forecast with different input data and actual wind fields is carried out. The results as illustrated in Table 3 are :

(*i*) The forecast wind fields with non-initialized initial data are amplified over the entire spectrum of motion and the total kinetic energy increases to almost three times that of the actual wind fields. Further though the zonal ($m=0$) and long waves are amplified to about two times, the synoptic scales and the high frequency gravity waves are amplified to more than 10 times the actual value and seem to be quite unrealistic.

(*ii*) The forecast kinetic energy (wind fields), with 6 hours initialized fields as input variables, improves considerably as the total kinetic energy does not exceed by more than 25% of the actual.

(*iii*) The kinetic energy of the actual and the forecast (which started with 18 hours initialized meteorological variables as input data) fields, are very close over the entire spectrum of waves and the total kinetic energy does not differ by more than 10% of the actual. However, in this case, the total kinetic energy of the forecast variables is less than that of the actual fields. The discrepancy is found to be comparatively larger in synoptic and short wave spectrum. This may be due to the fact that during 18 hours initialization, the amplitudes of synoptic and short waves are considerably reduced (Table 1).

From these results, it may be inferred, that any imbalance in the initial fields deteriorates the accuracy of the forecast fields, and in particular the synoptic and short waves are unrealistically amplified.

5.3 *Smoothing and filtering of high frequency waves*

Numerical weather prediction, using finite difference integration schemes, leads to amplification of high frequency waves in the final product, mainly due to numerical errors and computational instabilities. This serious growth of very short waves may not lead to a catastrophic instability of the model, like that caused by non-initialized input data (as discussed in

TABLE 4

Results of spectral decomposition of KE of initial wind field (6 Nov' 73), actual wind field (7 Nov' 73), and forecast wind field with different filters (After 18 hr of initialization)

Wave No.	Initial 6 Nov' 73	24 hours forecast from 18 hr initialization						Actual 7 Nov' 73
		Without filter	With filter 1				With filter 2 $\alpha=0.3$ $\beta=0.07$ $T=4\triangle t$	
			$\beta=.11$ $T=4\triangle t$	$\beta=0.07$ $T=4\triangle t$	$\beta=0.04$ $T=4\triangle t$	$\beta=0.07$ $T=\triangle t$		
$m=0$ (Zonal k_0)	34.5	30.7	29.6	30.6	30.9	28.8	30.5	30.8
$m=1, 2$ (Long waves) $L\geqslant 3400$ km	6.9	5.3	5.0	5.0	5.1	4.9	4.8	7.3
$m=3, 6$ (Synoptic scale) $L\geqslant 1100$ km <3400 km	0.5	0.5	0.3	0.4	0.5	0.3	0.4	1.4
$m=7, 15$ (Short waves) $L\geqslant 420$ km <1100 km	0.2	0.3	0.1	0.1	0.1	0.1	0.1	0.6
$m=0, 15$ (Total k_t)	42.1	36.8	35.0	36.1	36.6	34.1	35.8	40.1
$\frac{k_0}{\text{Total } k_t}$	0.82	0.83	0.85	0.85	0.85	0.85	0.85	0.77

Section 5.2); however, the amplification may exceed the physical reality and obscure the forecast variables. Therefore, it is desirable to eliminate such high frequency components by using some sort of filtering or smoothing operators. A number of smoothing operators are developed by various authors (Shuman 1957, Shapiro 1970). In this work, we have demonstrated the role of space smoothing operators to suppress computational high frequency two grid length wave generated in the process of finite difference integration of the prediction model (Eqns. 1-3).

Following two filters are used as space smoothing operators in our experiments :

(*i*) *Filter A*

Smoothing process

$$X_i^*=(1-2\beta)\,X_i+\beta\,(X_{i-1}+X_{i+1})$$

De-smoothing process

$$X_i^{**}=(1+2\beta)\,X_i^*-\beta\,(X^*_{i-1}+X_i^*{}_{+1}) \qquad (12)$$

(*ii*) *Filter B*

Smoothing process

$$X_i^*=(1-2\alpha)\,X_i+\alpha\,(X_{i-1}+X_{i+1})$$

$$X_i^\circ=X_i-X_i^*$$

$$X_i^{\circ *}=(1-2\beta)\,X_i^\circ+\beta\,(X_i^\circ{}_{-1}+X_i^\circ{}_{+1})$$

De-smoothing process

$$X_i^{\circ **}=(1+2\beta)\,X_i^{\circ *}-\beta\,(\overset{*}{X}_{i-1}+\overset{*}{X}_{i+1}) \qquad (13)$$

$$X_i^{**}=X_i^*+X_i^{\circ **}$$

where, α and β are the filter parameters, 'i') the number of grid point in the rows or the columns of the grid array and the indices '*' and '**' refer to smoothed and de-smoothed meteorological variables. In case of filter A, the smoothing and de-smoothing operators are used directly to the forecast meteorological variables like the treatment of Shuman (1957), whereas in case of filter B, as a first guess, the smoothing and de-smoothing operators are applied to the difference of the actual forecast and the first guess. The response functions of the two filters for a sinusoidal function e^{iky} are respectively

$$R_A=1-16\beta^2\sin^4(\pi\triangle y/L) \qquad (14)$$

$$R_B=1-\alpha\beta^2\left[-20+2\cos\left(6\pi\frac{\triangle y}{L}\right)+\right.$$

$$\left.+30\cos\left(2\pi\frac{\triangle y}{L}\right)-12\cos\left(4\pi\frac{\triangle y}{L}\right)\right] \qquad (15)$$

Five numerical experiments have been carried out with these two filters for different values of the filter parameters as described in Table 4. These experiments are designed to find out the best possible filter, that is, to select a single filter with appropriate values of the empirical filter parameters and the periodicity of the application of smoothing and de-smoothing process during time integration of the forecasting model.

From Table 4, it is seen that filter 'A' with $\beta=.07$ and .04 and filter B with $\alpha=.3$, $\beta=.07$, used after every four steps of time integration, have a property of selective smoothing of short and synoptic wave spectrums, without any significant change of the large scale processes (the change in the amplitude of zonal spectrum of kinetic energy by use of filter does not exceed 1%). The suitability of these two filters is also supported by their theoretical response functions to different waves (Fig. 8). Further, as the filter 'A', in its realization on computer, takes about half of the time taken by filter B, in our study we have selected filter A with $\beta=.07$ and $T=4\triangle t$, as the desired filter for the numerical forecasting model. The comparison of the forecast geopotential field (Fig. 7), with the actual field (Fig. 5) and the forecast field without filter (Fig. 6), clearly demonstrate the need of the filter in the process of prediction, which retains all the broad features and smoothes out only very short waves. The evaluation parameters of Table 2, quantitatively confirm the above findings, that the use of filter in forecasting model, improves the quality of the forecast.

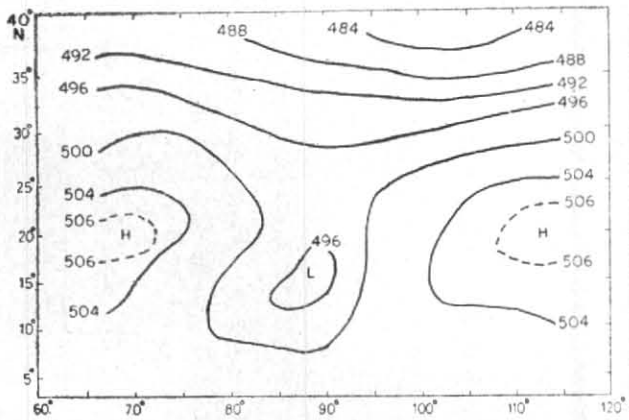

Fig. 5. The actual geopotential field (dkm) for 7 Nov' 73

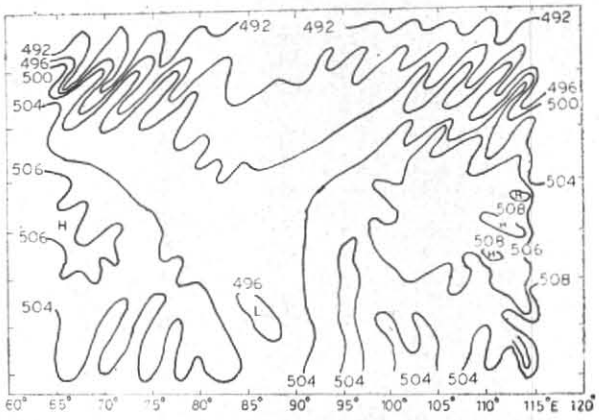

Fig. 6. 24 hours forecast geopotential (dkm) without smoothing obtained from 18 hours of initialized field of 6 Nov 1973

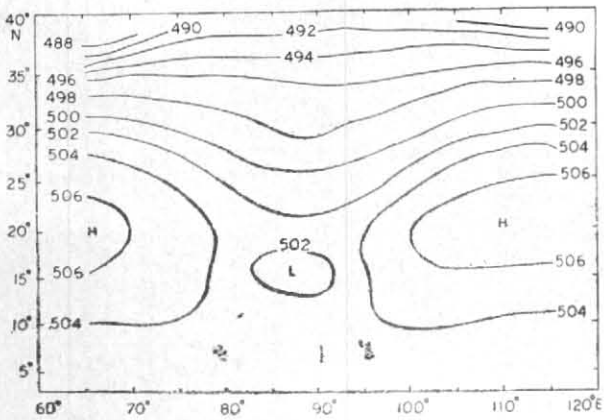

Fig. 7. 24 hours forecast geopotential (dkm) with smoothing (Filter 1) obtained from 18 hours of initialized field of 6 Nov 1973

TABLE 5

Results of vector error (δR in km) of the forecast of movement of cyclone and monsoon depression in the Bay of Bengal

Date	24-hr	48-hr
6 Nov'73	0	170
25 Nov'74	120	250
26 Nov'74	190	480
Mean	103	300
6 Jul'79	130	383

6. Forecasting the movement of tropical cyclones/monsoon depression in the Bay of Bengal

Finally after the complete development of the barotropic PE model (Eqns. 1-3) for tropics, as an outcome of various numerical experiments, conducted to study initial data problem in the tropics, an attempt is made to find out the applicability of this simple one level primitive equation model in forecasting the movement of tropical cyclones and monsoon depressions. For this purpose, three typical cases of post-monsoon cyclonic storms and a monsoon depression in the Bay of Bengal were considered. FGGE level IIIb data was utilized for the case of monsoon depression. To forecast the movement of the storm/depression, the total meteorological fields representing the complete synoptic situation, were integrated in time, by time integrating the model (Eqns. 1-3), allowing thereby free interaction between the vortex and its surrounding external influencing fields. The forecast fields were manually analysed to fix the new centre of the storm to be taken as the forecast position. The quantitative measure of vector difference (δR) between the forecast position and the actual position was found by evaluating $\delta R = \sqrt{(\delta x)^2 + (\delta y)^2}$, where δx and δy are the errors of displacement between the forecast position and the actual position along x-axis and y-axis respectively. Fig. 9 gives the actual and the predicted tracks of the monsoon depression.

The results of 24 hours and 48 hours forecasts are illustrated in Table 5. It is found that for the tropical storms, mean vector difference δR for 24 hours and 48 hours forecasts are 103 and 300 km respectively. For the monsoon depression, these values are 130 and 383 km respectively (Fig. 9). Considering the complexity of the problem from both the physical and the mathematical considerations, and also due to the inaccuracy in the determination of the initial and final position of the centre of the cyclone from the analysis of geopotential fields in the numerical experiments, the results seem to be quite reasonable (Sikka 1975, Singh and Saha 1976).

7. Conclusion

From the results of a number of numerical experiments with the barotropic PE model for the low latitudes, we may arrive at the following significant conclusions :

(*i*) In the low latitudes, the geopotential field can be derived from the observed wind fields with a

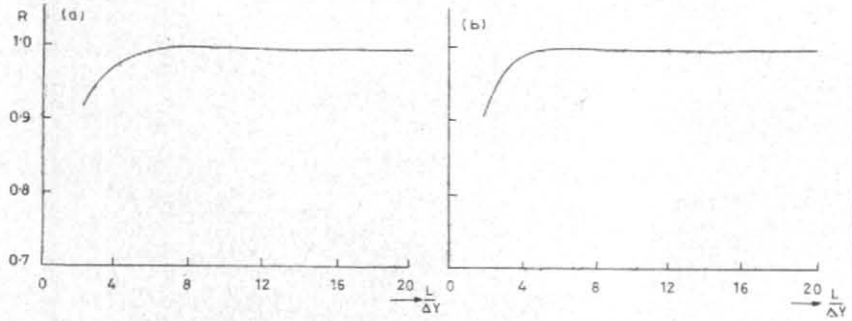

Fig. 8. Theoretical response function to different waves of : (a) Filter A for $\beta = .07$, $T = 4\triangle t$, (b) Filter B for $\alpha = .3$, $\beta = .07$, $T = 4\triangle t$

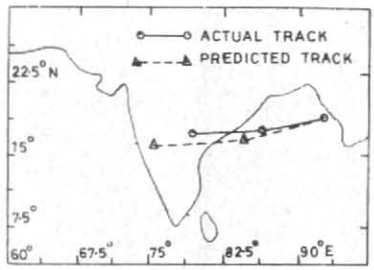

Fig. 9. Track of monsoon depression (6-8 July 1979)

considerable accuracy. Further, the observed wind fields seem to be a quite reasonable representation of the input data for a PE model.

(*ii*) Static initialization of the mass and the velocity field is not quite sufficient to suppress the spurious growth of high frequency inertia-gravity waves, in the process of time integration of PE model and thus the dynamic initialization of these meteorological variables is desirable.

(*iii*) The dynamic initialization exhibits the property of selective smoothing of high frequency wave spectrum. Further, the dynamic initialization does not change the broad features of the large scale processes and the centres of atmospheric vorticies (cyclones and anticyclones).

(*iv*) The dynamic initialization not only makes the model stable for a long time integration but also substantially improves the quality of forecast.

(*v*) Though dynamic initialization suppresses the high frequency modes, a space filter is of immense use to suppress the two grid wave to obtain a realistic forecast of the meteorological fields.

References

Cooley, J. W. and Tukey, J. W., 1965, 'An algorithm for the machine computation of complex fourier series', *Math. Comp.*, **19,** 297-301.

Das, P. K. and Bedi, H. S., 1978, 'The inclusion of Himalayas in a primitive equation model', *Indian J. Met. Hydrol. Geophys*; **29,** 375-383.

Falkovich, A. I., 1971, 'On retrieval of initial data in the low latitudes, *Met. & Hydrol.*, **12,** 18-24.

Gandin, L. S., 1963, 'Objective analysis of meteorological fields', *Guidromet. Izdaf.*, Leningrad, p. 287.

Gordan, C. T., Umscheid, L. and Miyakoda, K., 1972, 'Simulation experiments for determining wind data requirements in the tropics', *J. atmos. Sci.*, **29,** 1064-1075.

Houghton, D. and Washington, W ; 1969, 'On global initialization of the primitive equations', Part I, *J. appl. Met.*, **8,** 726-737.

Kivganov, A. F. and Mohanty, U. C., 1979, 'On the dynamic initialization of wind and geopotential fields in the low latitudes', *Met. & Hydrol.*, **8,** 40-48.

Krichak, S.O. 1976, 'Numerical experiments on forecasting meteorological fields over India by baroclinic equation model, *Trudi Hydromet. Centre*, USSR, **178**, 53-58.

Krishnamurti, T. N., 1969, 'An experiment in numerical weather prediction in equatorial latitudes,' *Quart. J. Roy. Met. Soc.*, **95,** 594-620.

Mohanty, U. C. and Flt. Lt. Madan, S. C., 1983, 'A numerical method for computing stream function and velocity potential from observed wind field', *Mausam*, **34,** 375-382.

Mohanty, U. C., 1982, 'Some characteristics of dynamical initialization of mass and velocity fields in the lower latitudes, *Mausam*, **33,** 29-34.

Nitta, T., Hovermale, J. B., 1969, 'A technique of objective analysis and initialization for the primitive forecast equations', *Mon. Weath. Rev.*, **97,** 652-658.

Obukhov, A. M., 1949, 'On the question of the geostrophic wind, *Izv. Akad. Nauk SSSR*, Ser Geograf. Geofiz, **13,** 281-306.

Sanders, F., Pike, S. C., Gaertner, J. P., 1975, 'A barotropic model for operational prediction of tracks of tropical storms', *J. appl. Met.*, **14,** 265-280.

Shapiro, R., 1970, 'Smoothing, filtering and boundary effects, *Rev. Geophys. and Space Phys.*, **8,** 359-387.

Shuman, F. G., 1957, 'Numerical methods in weather prediction—II : Smoothing and filtering', *Mon. Weath. Rev.*, **85,** 357-361.

Shuman, F. G. and Vanderman, L. W., 1969, 'Difference system and boundary conditions for the primitive equation barotropic forecast', Lectures on numerical short range weath. prediction, *Hydrometeoizdat*, Leningrad, 450-464.

Sikka, D. R., 1975, 'Forecasting the movement of tropical cyclone in the Indian Sea by non-divergent barotropic model', *Indian J. Met. Hydiol. Geophys.*, **26,** 323-325.

Singh, S. S. and Saha, K. R., 1976, 'Numerical experiments with a primitive equation barotropic model for the prediction of monsoon depressions and tropical cyclones', *J. appl. Met.*, **15,** 805-810.

Vanderman, L. W., 1969, 'Global forecast on a latitude-longitude grid with primitive equation models', Proc. Int. Sem. Trop. Meteor., Brazil.

Winninghoff, F. J., 1968, 'On the adjustment towards a geostrophic balance in a simple primitive equation model with application to the problems of initialization and objective analysis, Ph.D. thesis, Dept. Met., Univ. of California, Los Angeles.